

# Ring-Opening Polymerization of a Strained [3]Nickelocenophane: A Route to Polynickelocenes, a Class of $S = 1$ Metallopolymers

Sladjana Baljak,<sup>†</sup> Andrew D. Russell,<sup>†</sup> Samantha C. Binding,<sup>‡</sup> Mairi F. Haddow,<sup>†</sup> Dermot O'Hare,<sup>\*,‡</sup> and Ian Manners<sup>\*,†</sup>

<sup>†</sup>School of Chemistry, University of Bristol, Bristol BS8 1TS, United Kingdom

<sup>‡</sup>Chemistry Research Laboratory, Department of Chemistry, University of Oxford, Oxford OX1 3TA, United Kingdom

## Supporting Information

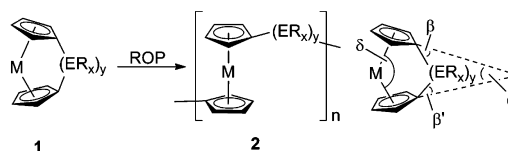
**ABSTRACT:** We report the synthesis, reactivity studies, and ring-opening polymerization of a tricarba[3]nickelocenophane. The resulting green polynickelocene (**5**) possesses a  $-(\text{CH}_2)_3-$  spacer between the nickelocene units and is shown to be of high molecular weight. SQUID magnetometry measurements indicate that **5** is a macromolecular material with an  $S = 1$  repeat unit.

Polymers containing metal centers as part of the main-chain or side-group structure are attractive targets because of their potential applications as functional soft materials.<sup>1</sup> Strained metallocenophanes (**1**) and their analogues with related  $C_x$  ( $x = 4-7$ )  $\pi$ -hydrocarbon ligands have attracted substantial attention<sup>2</sup> for their use as monomers in ring-opening polymerization (ROP) reactions to yield high-molecular-weight main-chain metal-containing polymers (e.g. **2**) (Scheme 1). The strain present in the monomer, which acts as a thermodynamic driving force for ring-opening, is related to the tilt angle  $\alpha$  in addition to other structural parameters (see Scheme 1, right).<sup>2b,d</sup> ROP of strained [ $n$ ]metallocenophanes has been shown to provide an excellent route to a broad variety of polymers, including well-defined architectures such as block copolymers.<sup>3</sup> In particular, polyferrocenylsilanes (**2**,  $M = \text{Fe}$ ,  $E = \text{Si}$ ,  $x = 2$ ,  $y = 1$ ), prepared by ROP of silicon-bridged [1]ferrocenophanes, have been extensively developed and have attracted interest as redox-responsive films, gels, and capsules,<sup>4</sup> nanostructured magnetic film precursors,<sup>5</sup> etch resists for nanolithography,<sup>6</sup> and patternable sources of carbon nanotube growth catalysts.<sup>7</sup>

Metallopolymers based on other metals such as Ti, V, Cr, and Ru have also been prepared by ROP of strained precursors, but these materials have only been briefly studied to date.<sup>8</sup> Very few examples of strained species and their corresponding ring-opened polymers based on late transition metals from group 9 or 10 have been described. We recently described ROP of a dicarba[2]cobaltocenophane to yield metallopolymers with main-chain Co centers.<sup>9-11</sup> Here we report ROP of a strained nickelocenophane and preliminary studies of the resulting polynickelocene, an unusual soluble polymer with two unpaired electrons on every main-chain metal center.

Nickelocene, which possesses 20 valence electrons (VEs), is a paramagnetic compound with a triplet ( $^3A_2$ ) ground state. The accommodation of two electrons in molecular orbitals with antibonding character results in a weaker and elongated Ni–Cp bond (mean Ni–C bond length = 2.178 Å)<sup>12</sup> in comparison to

**Scheme 1. Ring-Opening Polymerization of [ $n$ ]Metallocenophane **1** To Afford Metallopolymer **2**, and Structural Metrics of **1** (Right)**



both cobaltocene [19 VE, mean Co–C bond length = 2.119(3) Å]<sup>13</sup> and ferrocene [18 VE, mean Fe–C bond length = 2.064(3) Å].<sup>14</sup> These observations suggest that nickelocenophanes should be more tilted and strained than their direct Co and Fe analogues, with the same bridging moiety.<sup>15</sup>

Indeed, our attempts to prepare a strained dicarba[2]nickelocenophane via the same “fly trap” route employed previously to successfully prepare the Co analogue,<sup>11</sup> involving the reaction of dilithiated  $\text{Li}_2[(\text{C}_3\text{H}_4)_2(\text{CH}_2)_2]$  with  $\text{MCl}_2$  ( $-20^\circ\text{C}$ , THF,  $M = \text{Co}, \text{Ni}$ ), were unsuccessful in this case (see SI for details). Presumably this dicarba[2]nickelocenophane is too highly strained and labile to be synthesized.<sup>16</sup> However, it was found that the corresponding tricarba[3]nickelocenophane (**3**) could be successfully synthesized via an analogous method through the reaction of  $\text{Li}_2[(\text{C}_3\text{H}_4)_2(\text{CH}_2)_3]$  with  $\text{NiCl}_2$  ( $-20^\circ\text{C}$ , THF). Following workup by sublimation and recrystallization from hexanes at  $-40^\circ\text{C}$ , the product was isolated as a dark green crystalline solid in 17% yield.

The identity of **3** was supported by paramagnetic  $^1\text{H}$  NMR spectroscopy, which revealed broad peaks at  $-246.4$  and  $-272.2$  ppm, assigned to the  $\alpha$ - and  $\beta$ -protons of the cyclopentadienyl rings, respectively, and a peak at  $-29.4$  ppm for the  $\beta$ - $\text{CH}_2$  moiety (Figure S1). A resonance for the  $\alpha$ - $\text{CH}_2$  group was not detected, a situation that has precedent in other nickelocene derivatives.<sup>15a</sup> Overall, the data are broadly in line with those previously reported for *ansa*-nickelocenes, nickelocene, and its substituted analogues.<sup>15,17</sup> High-resolution MS and elemental analysis were also consistent with the assigned structure.

Single crystals of **3** suitable for X-ray diffraction were obtained by crystallization from *n*-hexane at  $-40^\circ\text{C}$  and the solid-state structure determined (Figure 1). The basic molecular geometry of **3** reveals the  $\text{C}_3\text{H}_4$  moieties to be bound to Ni in the expected  $\eta^5$ -fashion, similar to other [ $n$ ]nickelocenophanes<sup>15</sup> and nickel-

Received: February 14, 2014

Published: April 8, 2014

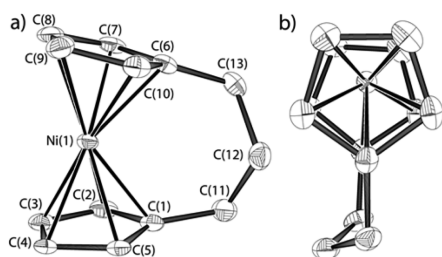


**Figure 1.** (a) Solid-state structure of tricarba[3]nickelocenophane (**3**) and (b) an alternative view. Thermal ellipsoids at the 50% probability level with H-atoms omitted for clarity. Selected bond lengths [Å] and angles [deg]: Ni1–Cp<sub>centroid</sub> = 1.805(1), C1–C11 = 1.510(3), C6–C13 = 1.503(3), C11–C12 = 1.534(3), C12–C13 = 1.532(3); C2–C1–C11 = 126.4(2), C1–C11–C12 = 115.7(2), C11–C12–C13 = 115.2(2).

ocene.<sup>12</sup> The distortion from coplanarity of the Cp ligands ( $\alpha$ ) is the largest so far reported for any (CH<sub>2</sub>)<sub>3</sub>-bridged [3]metallo-cenophane [ $\alpha$  = 16.6(1)°], significantly increased relative to the corresponding iron ( $\alpha$  = 10.30°),<sup>18</sup> cobalt [ $\alpha$  = 12.00(11)°],<sup>11</sup> and even ruthenium [ $\alpha$  = 14.8(2)°]<sup>19</sup> analogues. The angle  $\delta$  (Scheme 1) is consequently smaller in **3** [ $\delta$  = 166.3(1)°] than in both the iron (172.2°) and cobalt [171.0(5)°] species. The Cp<sub>centroid</sub>–C<sub>ipso</sub>–E angles ( $\beta/\beta'$ ) [6.8(2)/4.2(2)°] are broadly similar to those reported in the tricarba[3]ferrocenophanes (3.5/4.1°) and cobaltocenophanes [4.0(2)/3.5(14)°]. As anticipated, the Ni–Cp<sub>centroid</sub> distance [1.805(1) Å] is larger than the reported Fe–Cp<sub>centroid</sub> (1.637 Å) and Co–Cp<sub>centroid</sub> [1.718(2) Å] distances, which is consistent with the aforementioned trend observed for the corresponding metallocenes. These observations suggest that **3** has increased molecular strain relative to the previously reported tricarba[3]metallo-cenophane analogues.

The electronic structure of **3** was studied by solution visible spectroscopy (in THF, Figure S2) using nickelocene and 1,1'-dimethylnickelocene, Ni( $\eta^5$ -C<sub>5</sub>H<sub>4</sub>Me)<sub>2</sub>, as reference compounds. Interestingly, the lowest energy absorption for **3** (673 nm,  $\epsilon$  = 220 M<sup>-1</sup> cm<sup>-1</sup>) is hypsochromically shifted compared to those of both nickelocene (695 nm,  $\epsilon$  = 48 M<sup>-1</sup> cm<sup>-1</sup>) and Ni( $\eta^5$ -C<sub>5</sub>H<sub>4</sub>Me)<sub>2</sub> (683 nm,  $\epsilon$  = 170 M<sup>-1</sup> cm<sup>-1</sup>). This is in contrast to the data reported for the strained metallocenophanes of Fe, Ru, and Co, which exhibit bathochromic shifts in comparison to their analogous tilt-free metallocenes.<sup>2b,11,20</sup> The increase in the molar extinction coefficient ( $\epsilon$ ) for compound **3**, relative to those for nickelocene and Ni( $\eta^5$ -C<sub>5</sub>H<sub>4</sub>Me)<sub>2</sub>, is consistent with a relaxation of the Laporte selection rules due to the decrease in molecular symmetry that occurs upon introduction of the *ansa*-bridge.

To probe the influence of the ring strain in **3** on its reactivity, reactions were carried out with phosphines and N-heterocyclic carbenes (NHCs).<sup>21</sup> Thus, reaction of **3** with 2 equiv. of diphenylphosphinoethane (dppe) (THF, 20 °C, 2 h) led to complete displacement of the *ansa*- $\pi$ -hydrocarbon ligand to form Ni(dppe)<sub>2</sub> (see SI for details). In contrast, the corresponding reaction with nickelocene, to form the same product, requires extended reaction times at elevated temperatures (24 h, 110 °C, toluene).<sup>22</sup> When **3** was reacted with an equimolar amount of 1,3-bis(2,4,6-trimethylphenyl)imidazol-2-ylidene (toluene, 20 °C, 15 min), a color change from blue to red was observed, with the deep-red carbene complex **4** subsequently isolated in 72% yield upon workup (Scheme 2). Species **4**, which was analyzed by <sup>1</sup>H NMR spectroscopy (Figure S3), possesses a ring-slipped structure, as confirmed by single-crystal X-ray diffraction (Figure 2), with a reduced hapticity coordination mode ( $\eta^5$  to  $\eta^1$ ) for one Cp ligand. An analogous product, [Ni(NHC)( $\eta^1$ -

## Scheme 2. Reaction of **3** with 1,3-Bis(2,4,6-trimethylphenyl)imidazol-2-ylidene To Afford Compound **4**

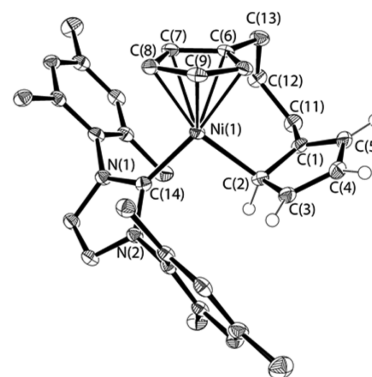
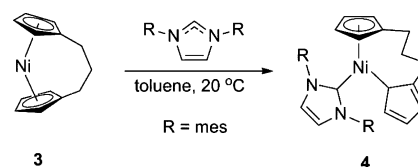
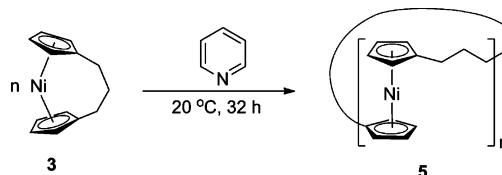


**Figure 2.** Solid-state structure of **4**. Thermal ellipsoids at the 50% probability level with most H-atoms omitted for clarity. Selected bond lengths [Å] and angles [deg]: Ni1–C2 = 2.032(2), Ni1–C14 = 1.900(2), Ni1–Cp<sub>centroid</sub> = 1.784(2); C2–Ni1–C14 = 97.16(10), Cp<sub>centroid</sub>–Ni1–C2 = 127.71(10), Cp<sub>centroid</sub>–Ni1–C14 = 134.98(9).

## Scheme 3. Polymerization of Tricarba[3]nickelocenophane (**3**) in Pyridine (20 °C, 32 h) To Yield Poly(nickelocenylpropylene) (**5**)



C<sub>5</sub>H<sub>5</sub>)( $\eta^5$ -C<sub>5</sub>H<sub>5</sub>)], was previously reported from a reaction of nickelocene with a different NHC, and in that case similar reaction conditions were used.<sup>23</sup>

In an attempt to induce thermal ROP of **3**, this species was heated (80 °C, 20 h), affording a green material that swelled but did not dissolve in organic solvents. Elemental analysis was consistent with the composition [Ni( $\eta^5$ -C<sub>5</sub>H<sub>4</sub>)<sub>2</sub>(CH<sub>2</sub>)<sub>3</sub>]<sub>n</sub>; it is thus possible that the product is a polymeric material, either cross-linked or of very high molecular weight. Interestingly, when species **3** was stirred in pyridine (20 °C, 32 h), the solution changed color from blue to green, consistent with the release of molecular strain. Solvent removal followed by precipitation from a concentrated THF solution into hexanes gave poly(nickelocenylpropylene) (**5**) (Scheme 3) as an organic-solvent-soluble, green solid in 68% yield. The paramagnetic <sup>1</sup>H NMR spectrum of **5** displayed broad peaks at 173.8 and 10.3 ppm (Figure S4), assigned to the  $\alpha$ - and  $\beta$ -protons of the -(CH<sub>2</sub>)<sub>3</sub>-spacer, respectively. A broad absorption (peak width at half-height = 1140 Hz) at –254.2 ppm was assigned to the two overlapping Cp environments. Characterization of **5** was also achieved by MALDI-TOF MS, dynamic light scattering (DLS), and visible spectroscopy.

MALDI-TOF analysis of **5** (Figure 3) indicated the presence of cyclic species up to 33 repeat units (7557 *m/z*). Assuming a

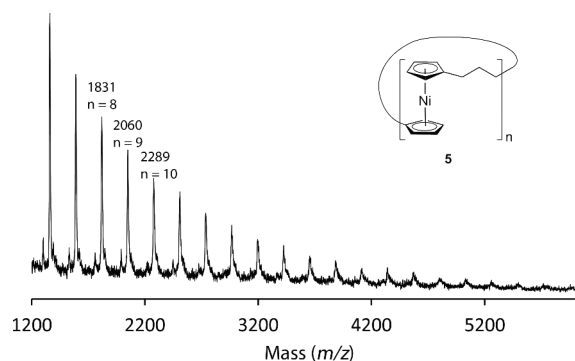


**Figure 3.** MALDI-TOF spectrum of **5**. The labels above the peaks correspond to the mass ( $m/z$ ) and degree of polymerization (DP).

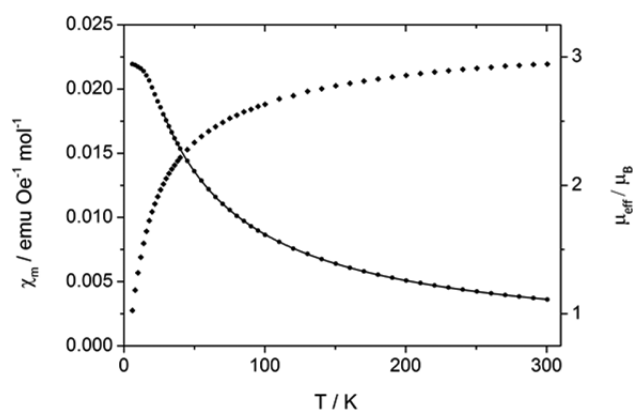


**Figure 4.** Temperature dependence of magnetic susceptibility ( $\chi_{\text{molNi}}$ ) and effective magnetic moment ( $\mu_{\text{eff}}$  per Ni) of poly(nickelocenyl-propylene) (**5**). Solid line shows the fit to eq 1 between 28 and 300 K.

M–Cp bond cleavage mechanism similar to that reported for ROP of [1]ferrocenophanes in the presence of light,<sup>3d</sup> these results suggest that the substitutionally labile pyridine initiator can be displaced from the coordination sphere of the Ni center by the Cp<sup>−</sup> end group. This “back-biting” reaction to form cyclic polymeric species has precedent in the photooligomerization of a sila[1]ferrocenophane in the presence of N-donors.<sup>24</sup> We presume that the higher lability of the Ni–Cp bond in the present case makes photoexcitation unnecessary.<sup>3d</sup> Interestingly, a second minor fraction is also observed in the MALDI-TOF spectrum of **5** (Figure S5), corresponding to linear polymer bearing two pyridine units at one end, suggesting that incomplete “back-biting” occurs during the polymerization.

DLS was conducted on polymer **5** (THF, 25 °C) at two different concentrations (Figure S6). In each case a single peak was observed corresponding to a hydrodynamic radius of  $R_h = 5.2$  nm.<sup>25</sup> For comparison, poly(ferrocenyldimethylsilane), with a weight-average molecular weight ( $M_w$ ) of 42 800 determined by static light scattering in THF, has a hydrodynamic radius of 5.3 nm.<sup>26</sup> This suggests a molecular weight for **5** of ca. 40 000, corresponding to a weight-average degree of polymerization ( $DP_w$ ) of 175. The data indicate that MALDI-TOF detects only the low-molecular-weight fraction of **5**. It is likely that the higher molecular weight material is richer in the linear component.

Visible spectroscopic analysis of **5** (THF) revealed a bathochromic shift of the lowest energy absorbance (to  $\lambda_{\text{max}} = 680$  nm) and a decrease of the extinction coefficient ( $\epsilon = 117 \text{ M}^{-1} \text{ cm}^{-1}$ ) (Figure S7) relative to those of **3**, which is consistent with ring-opening of nickelocenophanes.<sup>2b,20b</sup> Thermal gravimetric

analysis of **5** indicated a high char yield for an uncross-linked polymer (76% at 600 °C) (Figure S8).

Polynickelocene **5** represents an example of a soluble magnetic polymer composed of  $S = 1$  monomer units. SQUID magnetometry was used to measure the solid-state magnetic susceptibility of **5** between 6 and 300 K, and consequently we were able to determine the magnetic susceptibility per nickelocenyl repeat unit (see SI for details). Above 28 K the polymer behaves as a simple paramagnet. No difference in the zero-field-cooled and field-cooled magnetic susceptibility was observed, and the magnetic susceptibility per monomer unit ( $\chi_{\text{molNi}}$ ) can be fitted to the Curie–Weiss law plus a small additional term for a temperature-independent paramagnetic contribution,  $\chi_{\text{TIP}}$  (eq 1).

$$\chi_{\text{molNi}} = \frac{N\mu_{\text{eff}}^2}{3k_{\text{B}}(T - \theta)} + \chi_{\text{TIP}} \quad (1)$$

Least-squares fitting of the high-temperature magnetic susceptibility data to eq 1 gives an effective magnetic moment ( $\mu_{\text{eff}}$ ) per nickelocene of  $2.94 \mu_{\text{B}}$ , with  $\theta = -37$  K and  $\chi_{\text{TIP}} = 1.68 \times 10^{-4} \text{ emu G}^{-1} \text{ mol}^{-1}$  (Figure 4). The magnetic moment agrees very closely with the high-temperature effective magnetic moment found for molecular nickelocenes ( $\mu_{\text{eff}} = 2.88\text{--}2.92 \mu_{\text{B}}$ ).<sup>15c,27</sup> The large negative Weiss constant ( $\theta$ ) suggests significant antiferromagnetic spin–spin interactions. In contrast, extrapolation of the high-temperature magnetic susceptibility data for nickelocene indicates a very small Weiss constant.<sup>27c</sup>

The magnetic susceptibility for **5** deviates significantly from simple Curie–Weiss paramagnetic behavior below 28 K. We have investigated if this deviation may be ascribed to intramolecular spin–spin coupling within the polymer chains or to zero-field splitting of the  $^3A_2$  ground state of the nickelocenyl monomer. An excellent fit to the low-temperature magnetic susceptibility data can be obtained using the Fisher function for an infinite 1D chain of  $S = 1$  units,<sup>28</sup> with additional terms for  $\chi_{\text{TIP}}$ , and a small amount of a paramagnetic impurity (Figure S9), giving  $g = 1.891(7)$ ,  $J = -7.19(7)$  K,  $C = 0.023(1)$  K. This approach assumes that temperatures are sufficiently high for anisotropy to be insignificant and that interchain interactions are negligible to a first approximation. On the other hand, the solid-state magnetic susceptibility studies of nickelocene show that it exhibits a large-zero-field splitting with  $D = 25.4 \text{ cm}^{-1}$ .<sup>27c</sup> Performing a similar analysis on the magnetic susceptibility of **5**,<sup>27c</sup> the magnetic susceptibility data were fitted to eq 2, which assumes the magnetic center has axial symmetry.

$$\chi_{\text{molNi}} = \frac{2}{3}N\mu_{\text{B}}^2 \left[ \frac{g_{\parallel}^2}{k_{\text{B}}(T - \theta)} \frac{\exp(-D/k_{\text{B}}T)}{1 + 2 \exp(-D/k_{\text{B}}T)} + \frac{2g_{\perp}^2}{D} \frac{1 - \exp(-D/k_{\text{B}}T)}{1 + 2 \exp(-D/k_{\text{B}}T)} \right] + \chi_{\text{TIP}} \quad (2)$$

Least-squares fitting to eq 2 over the entire temperature range (6–300 K) and assuming a spin-only value for  $g_{\parallel}$  ( $2.0023$ )<sup>27c</sup> yields  $g_{\perp} = 2.32$ ,  $\theta = -40.2$  K, and  $D = 84.4 \text{ cm}^{-1}$  (Figure S10). The Weiss constant is unusually high for a paramagnetic molecular metallocene, indicating the possibility of some intrachain interactions, while the zero-field splitting is consistent with an isolated nickelocene-type system. At present the



magnetic susceptibility data for **5** do not allow us to unambiguously determine the nature of all the spin–spin interactions.

In summary, we report a ROP route to soluble magnetic polynickelocenes. Future work will focus on understanding the ROP mechanism, controlling the formation of linear or cyclic material and the formation of crystalline forms of the polymer. Access to samples with aligned polymer chains may allow for more well-defined interactions between the Ni spin centers and more substantial cooperative magnetic behavior.

## ■ ASSOCIATED CONTENT

### Supporting Information

Experimental details and characterization data. This material is available free of charge via the Internet at <http://pubs.acs.org>.

## ■ AUTHOR INFORMATION

### Corresponding Authors

dermot.ohare@chem.ox.ac.uk  
ian.manners@bris.ac.uk

### Notes

The authors declare no competing financial interest.

## ■ ACKNOWLEDGMENTS

S.B., A.D.R., and I.M. thank the EU for funding. S.C.B. and D.O'H. thank SCG Chemicals, Thailand, for financial support.

## ■ REFERENCES

- (1) (a) Heilmann, J. B.; Scheibitz, M.; Qin, Y.; Sundararaman, A.; Jäkle, F.; Kretz, T.; Bolte, M.; Lerner, H. W.; Holthausen, M. C.; Wagner, M. *Angew. Chem., Int. Ed.* **2006**, *45*, 920. (b) Chan, W. K. *Coord. Chem. Rev.* **2007**, *251*, 2104. (c) Gohy, J.-F. *Coord. Chem. Rev.* **2009**, *253*, 2214. (d) Miles, D.; Ward, J.; Foucher, D. A. *Macromolecules* **2009**, *42*, 9199. (e) Powell, A. B.; Bielawski, C. W.; Cowley, A. H. *J. Am. Chem. Soc.* **2009**, *131*, 18232. (f) Ren, L.; Hardy, C. G.; Tang, C. *J. Am. Chem. Soc.* **2010**, *132*, 8874. (g) Chadha, P.; Ragogna, P. J. *Chem. Commun.* **2011**, *47*, 5301. (h) Ho, C.-L.; Wong, W.-Y. *Coord. Chem. Rev.* **2011**, *255*, 2469. (i) Whittell, G. R.; Hager, M. D.; Schubert, U. S.; Manners, I. *Nat. Mater.* **2011**, *10*, 176. (j) Wang, X.; Cao, K.; Liu, Y.; Tsang, B.; Liew, S. *J. Am. Chem. Soc.* **2013**, *135*, 3399. (k) Zhang, J.; Yan, Y.; Chance, M. W.; Chen, J.; Hayat, J.; Ma, S.; Tang, C. *Angew. Chem., Int. Ed.* **2013**, *52*, 13387.
- (2) (a) Tamm, M.; Kunst, A.; Bannenberg, T.; Herdtweck, E.; Sirsch, P.; Elsevier, C. J.; Ernsting, J. M. *Angew. Chem., Int. Ed.* **2004**, *43*, 5530. (b) Herbert, D. E.; Mayer, U. F. J.; Manners, I. *Angew. Chem., Int. Ed.* **2007**, *46*, 5060. (c) Braunschweig, H.; Kupfer, T. *Acc. Chem. Res.* **2010**, *43*, 455. (d) Musgrave, R. A.; Russell, A. D.; Manners, I. *Organometallics* **2013**, *32*, 5654.
- (3) (a) Foucher, D. A.; Tang, B.-Z.; Manners, I. *J. Am. Chem. Soc.* **1992**, *114*, 6246. (b) Temple, K.; Jäkle, F.; Sheridan, J. B.; Manners, I. *J. Am. Chem. Soc.* **2001**, *123*, 1355. (c) Mizuta, T.; Imamura, Y.; Miyoshi, K. *J. Am. Chem. Soc.* **2003**, *125*, 2068. (d) Tanabe, M.; Vandermeulen, G. W. M.; Chan, W. Y.; Cyr, P. W.; Vanderark, L.; Rider, D. A.; Manners, I. *Nat. Mater.* **2006**, *5*, 467. (e) Bellas, V.; Rehahn, M. *Angew. Chem., Int. Ed.* **2007**, *46*, 5082. (f) Bagh, B.; Gilroy, J. B.; Staubitz, A.; Müller, J. *J. Am. Chem. Soc.* **2010**, *132*, 1794.
- (4) (a) Espada, L.; Pannell, K. H.; Papkov, V.; Leites, L.; Bukalov, S.; Suzdalev, I.; Tanaka, M.; Hayashi, T. *Organometallics* **2002**, *21*, 3758. (b) Ma, Y.; Dong, W.-F.; Hempenius, M. A.; Möhwal, H.; Vancso, G. J. *Nat. Mater.* **2006**, *5*, 724. (c) Puzzo, D. P.; Arsenaull, A. C.; Manners, I.; Ozin, G. A. *Angew. Chem., Int. Ed.* **2009**, *48*, 943. (d) Sui, X.; Hempenius, M. A.; Vancso, G. J. *J. Am. Chem. Soc.* **2012**, *134*, 4023.
- (5) Rider, D. A.; Liu, K.; Eloi, J.-C.; Vanderark, L.; Yang, L.; Wang, J.-Y.; Grozea, D.; Lu, Z. H.; Russell, T. P.; Manners, I. *ACS Nano* **2008**, *2*, 263.
- (6) (a) Korczagin, I.; Lammertink, R. G. H.; Hempenius, M. A.; Golze, S.; Vancso, G. J. *Adv. Polym. Sci.* **2006**, *200*, 91. (b) Chuang, V. P.;

Gwyther, J.; Mickiewicz, R. A.; Manners, I.; Ross, C. A. *Nano Lett.* **2009**, *9*, 4364.

(7) (a) Ginzburg, M.; MacLachlan, M. J.; Yang, S. M.; Coombs, N.; Coyle, T. W.; Raju, N. P.; Greedan, J. E.; Herber, R. H.; Ozin, G. A.; Manners, I. *J. Am. Chem. Soc.* **2002**, *124*, 2625. (b) Lu, J. Q.; Kopley, T. E.; Moll, N.; Roitman, D.; Chamberlin, D.; Fu, Q.; Liu, J.; Russell, T. P.; Rider, D. A.; Manners, I.; Winnik, M. A. *Chem. Mater.* **2005**, *17*, 2227.

(8) (a) Nelson, J. M.; Lough, A. J.; Manners, I. *Angew. Chem., Int. Ed.* **1994**, *33*, 989. (b) Berenbaum, A.; Manners, I. *Dalton Trans.* **2004**, 2057. (c) Vogel, U.; Lough, A. J.; Manners, I. *Angew. Chem., Int. Ed.* **2004**, *43*, 3321. (d) Braunschweig, H.; Adams, C. J.; Kupfer, T.; Manners, I.; Richardson, R. M.; Whittell, G. R. *Angew. Chem., Int. Ed.* **2008**, *47*, 3826. (e) Tamm, M. *Chem. Commun.* **2008**, 3089. (f) Bagh, B.; Schatte, G.; Green, J. C.; Müller, J. *J. Am. Chem. Soc.* **2012**, *134*, 7924. (g) Tagne Kuate, A. C.; Daniliuc, C. G.; Jones, P. G.; Tamm, M. *Eur. J. Inorg. Chem.* **2012**, *2012*, 1727.

(9) (a) Mayer, U. F. J.; Gilroy, J. B.; O'Hare, D.; Manners, I. *J. Am. Chem. Soc.* **2009**, *131*, 10382. (b) Gilroy, J. B.; Patra, S. K.; Mitchels, J. M.; Winnik, M. A.; Manners, I. *Angew. Chem., Int. Ed.* **2011**, *50*, 5851. (c) Qiu, H. B.; Gilroy, J. B.; Manners, I. *Chem. Commun.* **2013**, *49*, 42.

(10) For recent work on side-chain metallopolymer containing Co, see: Ren, L.; Hardy, C. G.; Tang, S.; Doxie, D. B.; Hamidi, N.; Tang, C. *Macromolecules* **2010**, *43*, 9304. In addition, see refs 1e, 1f, and 1j.

(11) Mayer, U. F. J.; Charmant, J. P. H.; Rae, J.; Manners, I. *Organometallics* **2008**, *27*, 1524. In addition, see refs 1f, 1g, and 1k.

(12) Seiler, P.; Dunitz, J. D. *Acta Crystallogr. Sect. B, Struct. Commun.* **1980**, *36*, 2255.

(13) Antipin, M. Y.; Boese, R.; Augart, N.; Schmid, G. *Struct. Chem.* **1993**, *4*, 91.

(14) Dunitz, J. D.; Orgel, L. E.; Rich, A. *Acta Crystallogr.* **1956**, *9*, 373.

(15) To our knowledge only three tilted *ansa* [*n*]nickelocenophanes (*n* = 2–4) have been reported, tetracarba[4]nickelocenophane ( $\alpha = 8^\circ$ ), disila[2]nickelocenophane ( $\alpha = 9^\circ$ ), and C<sub>3</sub>-naphthalene-bridged *ansa*-nickelocene ( $\alpha = 20^\circ$ ): (a) Buchowicz, W.; Jerzykiewicz, L. B.; Krasińska, A.; Losi, S.; Pietrzykowski, A.; Zanello, P. *Organometallics* **2006**, *25*, 5076. (b) Braunschweig, H.; Gross, M.; Radacki, K. *Organometallics* **2007**, *26*, 6688. (c) Trtica, S.; Meyer, E.; Proscen, M. H.; Heck, J.; Böhnert, T.; Görlitz, D. *Eur. J. Inorg. Chem.* **2012**, 4486.

(16) Insolubility of the crude reaction product from the attempted synthesis of the dicarba[2]nickelocenophane (see SI) was attributed to the formation of oligo- and polymeric species.

(17) Pasynkiewicz, S.; Pietrzykowski, A. *Coord. Chem. Rev.* **2002**, *231*, 199.

(18) Kadkin, O.; Nather, C.; Friedrichsen, W. *J. Organomet. Chem.* **2002**, *649*, 161.

(19) Ohba, S.; Saito, Y.; Kamiyama, S.; Kasahara, A. *Acta Crystallogr. Sect. C* **1984**, *C40*, 53.

(20) (a) Sohn, Y. S.; Hendrickson, D. N.; Gray, H. B. *J. Am. Chem. Soc.* **1970**, *92*, 3233. (b) Yamaguchi, Y.; Ding, W.; Sanderson, C. T.; Borden, M. L.; Morgan, M. J.; Kutal, C. *Coord. Chem. Rev.* **2007**, *251*, 515.

(21) For reactions of NHCs with other metallocenes, see: Abernethy, C. D.; Cowley, A. H.; Jones, R. A. *J. Organomet. Chem.* **2000**, *596*, 3, and references cited therein.

(22) Van Hecke, G. R.; Horrocks, D. W., Jr. *Inorg. Chem.* **1966**, *5*, 1968.

(23) Abernethy, C. D.; Clyburne, J. A. C.; Cowley, A. H.; Jones, R. A. *J. Am. Chem. Soc.* **1999**, *121*, 2329.

(24) Herbert, D. E.; Gilroy, J. B.; Chan, W. Y.; Chabanne, L.; Staubitz, A.; Lough, A. J.; Manners, I. *J. Am. Chem. Soc.* **2009**, *131*, 14958.

(25) The lack of concentration dependence for the DLS data was consistent with the presence of unimers rather than aggregates.

(26) Massey, J. A.; Kulbaba, K.; Winnik, M. A.; Manners, I. *J. Polym. Sci. Polym. Phys.* **2000**, *38*, 3032.

(27) (a) Fisher, E. O.; Jira, R. Z. *Naturforsch.* **1953**, *8b*, 217. (b) Wilkinson, G.; Pauson, P. L.; Cotton, F. A. *J. Am. Chem. Soc.* **1954**, *76*, 1970. (c) Prins, R.; Van Voorst, J. D. W.; Schinkel, C. J. *Chem. Phys. Lett.* **1967**, *1*, 54.

(28) Bonner, J. C.; Fisher, M. E. *Phys. Rev.* **1964**, *135*, A640.